

Dependence of the cross polar cap potential saturation on the type of solar wind streams

N. S. Nikolaeva,¹ Yu. I. Yermolaev,¹ I. G. Lodkina,¹

arXiv:1312.0778v1 [physics.space-ph] 3 Dec 2013

¹Space Plasma Physics Department,
Space Research Institute, Russian Academy
of Sciences, Profsoyuznaya 84/32, Moscow
117997, Russia. (nnikolae@iki.rssi.ru)

Abstract.

We compare of the cross polar cap potential (CPCP) saturation during magnetic storms induced by various types of the solar wind drivers. By using the model of Siscoe-Hill [*Hill et al.*, 1976; *Siscoe et al.*, 2002a, b, 2004; *Siscoe*, 2011] we evaluate criteria of the CPCP saturation during the main phases of 257 magnetic storms ($Dst_{min} \leq -50$ nT) induced by the following types of the solar wind streams: magnetic clouds (MC), Ejecta, the compress region Sheath before MC (Sh_{MC}) and before Ejecta (Sh_E), corotating interaction regions (CIR) and indeterminate type (IND). Our analysis shows that occurrence rate of the CPCP saturation is higher for storms induced by ICME (13.2%) than for storms driven by CIR (3.5%) or by IND (3.5%). The CPCP saturation was obtained more often for storms initiated by MC (25%) than by Ejecta (2.9%); it was obtained for 8.6% of magnetic storms induced by sum of MC and Ejecta, and for 21.5% magnetic storms induced by Sheath before them (sum of Sh_{MC} and Sh_E). These results allow us to conclude that occurrence rate of the CPCP saturation at the main phase of magnetic storms depends on the type of the solar wind stream.

1. Introduction

As well known the main cause of geomagnetic storms is solar wind electric field $E_y = V_x \times B_z$, where V_x is radial component of solar wind velocity and B_z is the southward component of interplanetary magnetic field (IMF). Solar wind includes various types of streams characterized by different behavior of strength and structure of IMF, density and velocity of solar wind, and these types of streams result in different forms of geomagnetic activity [*Boudouridis et al.*, 2004; *Borovsky and Denton*, 2006; *Huttunen et al.*, 2006; *Pulkkinen et al.*, 2007; *Yermolaev et al.*, 2007; *Plotnikov and Barkova*, 2007; *Longden et al.*, 2008; *Turner et al.*, 2009; *Despirak et al.*, 2011; *Nikolaeva et al.*, 2011; *Guo et al.*, 2011; *Yermolaev et al.*, 2012].

There are 5 geoeffective types/subtypes of the solar wind (SW): (1) Corotation Interaction Region (CIR), when high velocity stream of SW from coronal hole interacts with slow SW above the streamer belt; (2) Magnetic Clouds (MC), or well organized structures with enhanced IMF magnitude, large and smooth rotation of IMF vector over period ~ 1 day; low proton temperatures [*Burlaga et al.*, 1981]; (3) Ejecta, with less organized structure than MC; (4) Sheath or compression region before the leading edge of MC (Sh_{MC}); and (5) Sheath before Ejecta (Sh_E) (for example, see [*Yermolaev et al.*, 2009]).

The cross polar cap potential saturation is one of differences between CME- and CIR-induced geomagnetic storms [*Borovsky and Denton*, 2006]. It is known that potential across polar cap is increasing with growth of E_y . But sometimes its value does not change with increasing of E_y (i.e. it reaches the saturation threshold) under favorable solar wind conditions often associated with strong magnetic storms [*Reiff and Luhmann*,

1986; *Russell et al.*, 2000, 2001; *Nagatsuma*, 2002; *Shepherd et al.*, 2002; *Ober et al.*, 2003; *Hairston et al.*, 2003; *Boudouridis et al.*, 2004; *Hairston et al.*, 2005; *Borovsky and Denton*, 2006; *Shepherd*, 2007].

The cross polar cap potential saturation is confirmed experimentally (for example, [*Nagatsuma*, 2002; *Shepherd et al.*, 2002; *Hairston et al.*, 2003; *Ober et al.*, 2003]). Also this phenomena is agreed with MHD simulations [*Raeder et al.*, 2001; *Siscoe et al.*, 2002a; *Merkine et al.*, 2003]. For an explanation of CPCP saturation it was proposed several models, although the physical mechanism is still debated [*Siscoe et al.*, 2002a, b, 2004; *Kivelson and Ridley*, 2008; *Lavraud and Borovsky*, 2008; *Borovsky et al.*, 2009; *Gao et al.*, 2013].

The authors [*Borovsky et al.*, 2009] compare several models for explanation of CPCP saturation dividing them into two types: "reconnection models" and "postreconnection models". The reconnection models explain the reduction of CPCP by reduction in the reconnection rate at the dayside of the magnetosphere, i.e., by reduction of SW-magnetosphere coupling [*Hill et al.*, 1976; *Pudovkin et al.*, 1985; *Raeder et al.*, 2001; *Siscoe et al.*, 2002a; *Merkin et al.*, 2005a, b; *Raeder and Lu*, 2005; *Ridley*, 2005; *Hernandez et al.*, 2007]. The postreconnection models explain decreasing of CPCP by processes occurring after the solar wind plasma reconnects with magnetosphere [*Winglee et al.*, 2002; *Siscoe et al.*, 2002b; *Ridley*, 2007; *Kivelson and Ridley*, 2008]. From these models the authors [*Borovsky et al.*, 2009] choose the MHD-generator model [*Kivelson and Ridley*, 2008] as the best one because it agree with results of global MHD modeling.

The investigations (for example, [*Lavraud and Borovsky*, 2008; *Siscoe*, 2011] show that CPCP predicted by [*Siscoe et al.*, 2002b] is similar one predicted by [*Kivelson and Ridley*,

2008]. The similarities and differences between these two models were investigated in the work [Gao *et al.*, 2013]. The authors compare mathematical formulas and predictions of both models with data measurements. The results of the analysis show that both models predict similar saturation limits mathematically and give similar model predictions for CPCP value measured during time interval 1999–2009 [Gao *et al.*, 2013].

Authors of the works [Siscoe *et al.*, 2002a, b, 2004; Siscoe, 2011] on the basis of the hypothesis [Hill *et al.*, 1976], have developed a theoretical model of coupling between the solar wind and the magnetosphere and ionosphere, which predicts the CPCP saturation. It occurs, when the region I current system generates a magnetic field which is approximately equal to dipole field at the dayside magnetopause [Hill *et al.*, 1976; Siscoe *et al.*, 2002a, b, 2004; Siscoe, 2011]. Authors formulated the criterion of CPCP saturation which connects transpolar potential with the value of interplanetary electric field, solar wind dynamic pressure and ionospheric conductance [Siscoe *et al.*, 2002a, b, 2004; Siscoe, 2011].

According to numerous works [Hill *et al.*, 1976; Balan *et al.*, 1993; Siscoe *et al.*, 2002a, b; Ober *et al.*, 2003; Siscoe *et al.*, 2004; Floyd *et al.*, 2005; Borovsky and Denton, 2006] the saturation of the polar cap potential occurs when a saturation parameter:

$$Q = Va\Sigma_p/806 = VaF10.7^{1/2}/1050 > 2 \quad (1)$$

where Va is the Alfvén velocity in the solar wind, Σ_p is the height-integrated Pederson conductivity of the ionosphere; according the work [Robinson and Vondrak, 1984] its value can be determined as $\Sigma_p = 0.77F10.7^{1/2}$, where $F10.7$ is solar radio flux as proxy Σ_p (see details in papers by [Borovsky and Denton, 2006; Lavraud and Borovsky, 2008] and references therein).

Using OMNI2 data set authors [Borovsky and Denton, 2006] obtained that the saturation of polar cap potential (i.e. $Q > 2$) was usually observed for CME-driven storms, but rarely observed for CIR-driven magnetic storms. It should be noted that in accordance with author's definition the CME-driven magnetic storms include all storms initiated by various interplanetary manifestations of CME: sheath, ejecta, and magnetic cloud [Borovsky and Denton, 2006]. Note that authors [Borovsky and Denton, 2006] used international sunspot number $S_n^{1/2}$ (with time resolution 1 month) as proxy Σ_p .

In contrast to previous papers we separately study magnetic storms induced by various components of CME manifestations. Also as proxy Σ_p we used the solar radio flux $F_{10.7}$ which correlates with S_n value, but gives more real values for Σ_p [Ober et al., 2003].

The main aim of our work is an estimation of the CPCP saturation during the main phase of magnetic storms induced by different types of the solar wind streams which include CIR, and separately types of ICME such as magnetic clouds (MC), Ejecta, and Sheath before them (Sh_{MC} and Sh_E , respectively). Separation of Sheath-storms on 2 types Sh_{MC} and Sh_E is partly justified by one of the results of the work [Nikolaeva et al., 2011]. Magnetic storms induced by Sh_{MC} have lower value of Dst_{min} and higher value of AE index.

In given work we analyze different types of magnetic storms (including their subtypes) in order to estimate what types/subtypes of SW more often lead to non-linear type of interaction with magnetosphere-ionosphere system (which manifests itself in CPCP saturation). In addition we used solar radio flux at 10.7 cm (with time resolution 1 day) as proxy Σ_p .

2. Data

For our analysis we use OMNI data of interplanetary parameters and the "The Catalog of Large-scale Solar Wind Phenomena during 1976–2000" (site <ftp://ftp.iki.rssi.ru/pub/omni/>) [*King and Papitashvili, 2005; Yermolaev et al., 2009*]. The method of identification of different types of SW on the basis of plasma and magnetic field data is described in detail in the work [*Yermolaev et al., 2009*]. The technique of determination of connection between magnetic storms and their interplanetary drivers is the following. If the minimum of Dst index lies in an interval of a type of solar wind streams or is observed within 1–2 hours after it we believe that the given storm has been generated by the given type of streams [*Yermolaev et al., 2010*].

To calculate the saturation parameter Q for different drivers we select 257 magnetic storms with $Dst \leq -50$ nT and with full set of solar wind parameters needed for calculation of parameter according relation (1). The solar wind data for calculation of Alfvén velocity Va and solar radio flux $F10.7^{1/2}$, which used as proxy Σ_p , were received from OMNI data base [*King and Papitashvili, 2005*].

The following types of the solar wind streams are sources of the magnetic storms: corotating interaction regions, CIR – 56 magnetic storms; magnetic clouds, MC – 24 magnetic storms; the compression regions ahead MC, Sh_{MC} – 5 events; Ejecta – 69 events; the compression regions ahead Ejecta, Sh_E – 46 events, and indeterminate type IND (the sources which are impossible to determine because of data gap) – 57 events. To compare results of this paper with previous results [*Borovsky and Denton, 2006*] we calculate similar parameters for sum of subtypes of ICME, magnetic clouds MC and Ejecta (MC+Ejecta)

– 93 magnetic storms, and compression regions before them Sheath ($Sh_{MC} + Sh_E$) – 51 magnetic storms.

3. Results

Figure 1 shows the distribution of 257 magnetic storms with $Dst \leq -50$ nT in dependence on type of the solar wind driver. We see that only 22% of storms driven by CIR, but 56% of all storms are driven by sum $MC + Ejecta + Sheath$ (including 36% storms driven by sum $(MC + Ejecta)$ and 20% storms driven by Sheath $(Sh_{MC} + Sh_E)$ ahead $(MC + Ejecta)$).

The results of evaluation of saturation parameter Q and corresponding solar wind parameters: Alfvén velocity Va and the solar radio flux $F10.7^{1/2}$, which are included in the formula (1) for Q , are presented in Figure 2. In the Figure 2 the occurrence distribution of the polar cap saturation parameter Q is binned according type of solar wind drivers (top panel). In the middle and bottom panels in Figure 2 the Alfvén velocity Va and solar radio flux $F10.7^{1/2}$ are binned, respectively.

The following designations are used for different types of magnetic storms (in Figure 2 a, c, e): thick blue line for CIR, thin blue line for IND, solid brown line for MC, dotted brown line for Sh_{MC} , solid red line for Ejecta, dotted red line for Sh_E , solid purple line for sum of $MC + Ejecta$, and dotted purple line for sum $Sh_{MC} + Sh_E$, or Sheath. The right panels (b, d, f) in Figure 2 present the same data as in the left panels, but all magnetic storms are selected only into 3 main types of drivers as it was made in work by [Borovsky and Denton, 2006]: (1) CIR (thick grey line), (2) MC (thin black line), (i.e., CIR and MC repeat that on the left in Figure 1), and (3) ICME, which includes all of the interplanetary manifestations of CME: magnetic clouds (MC) and Ejecta, also the compression region

Sheath (i.e. sum of $MC + Ejecta + Sheath$). This type is close to CME-driven storms in paper [Borovsky and Denton, 2006] and below we compare them. The right panels (b, d, f) in Figure 2 permit to compare our results with other works.

In Table 1 there are presented average and median values of Alfvén velocity Va , parameter of saturation Q , and $F10.7^{1/2}$ (as proxy Σ_p) for different types of SW drivers. We can see that MC- and Sh_{MC} - storms have the highest values of Q , Va , $F10.7^{1/2}$; while CIR-, and IND-storms have the lowest ones with factors 2, 1.7, 1.3, respectively.

Median values of Q depend on type of magnetic storms and change (in 2.8-1.8 times) from maximal values 2.4 and 1.53 (for Sh_{MC} - and MC- storms, respectively), to minimal values of 0.91 and 0.85 (for IND- and CIR- storms, respectively). The median value Q is higher for Sh_{MC} - storms than for MC-storms (factor 1.6). In our sample of storms the factor between median values Q for MC- and CIR- storms is equal 1.8 (against 2.9, in [Borovsky and Denton, 2006]). The median value of Q for CME-driven storms given by [Borovsky and Denton, 2006] is lower with factor 1.4 in comparison with Q for ICME-driven storms (see Table 1 and Figure 2b). Such discrepancy may be explained by different events statistics in samples and by using $Sn^{1/2}$ as proxy Σ_p .

The median values Va are changing between maximum values 145 and 112 km/s for ShE- and MC-storms, respectively, and minimal values 70 and 78 km/s for IND-storms and CIR- and Ejecta- storms, respectively. For storms induced by (MC+Ejecta) and by compression region Sheath ($= Sh_{MC} + Sh_E$) the median values Va are very close (98.6 and 96 km/s, respectively). For storms induced by MC and Sh_{MC} the factor between median values Va is 1.3. The work [Borovsky and Denton, 2006] contains the following

median values of Va: 78 km/s for CIR-storms and 131 km/s for MC- storms and 95 km/s for CME- driven storms. These values are close to our results.

The highest median values of solar radio flux $F10.7^{1/2} = 16$ are associated with Sh_{MC} - storms, the lowest values $F10.7^{1/2} = 12.5$ and 12.8 have storms induced by CIR and IND (factor 1.3). The magnetic storms induced by MC+Ejecta and by Sheath have equal median values $F10.7^{1/2} = 13.5$. But Sh_{MC} - storms have the median values $F10.7^{1/2} = 16$ larger than for MC-storms $F10.7^{1/2} = 13.45$ (with factor 1.2). In work [Borovsky and Denton, 2006] there are presented following median values of $Sn^{1/2}$ (used as proxy Σ_p): for CIR-storms $Sn^{1/2} = 4.8$ (relative to our median value $F10.7^{1/2} = 12.5$), for MC- storms $Sn^{1/2} = 8.7$ (our median value $F10.7^{1/2} = 13.4$), for CME-storms $Sn^{1/2} = 9.9$ (our median value $F10.7^{1/2} = 13.55$). So the range of conductivity changing is equal 1.3 in our work (when solar radio flux $F10.7^{1/2}$ as proxy Σ_p), in respect to factor 2 in work [Borovsky and Denton, 2006], in which sunspot number $Sn^{1/2}$ was used as proxy conductivity.

In Table 2 there are presented the number of magnetic storms driven by various types of SW for 3 levels of saturation parameter Q. It is seen that high value of saturation parameter $Q > 2$ was observed in 3.8 times more often for storms driven by ICME than by CIR and IND; also parameter $Q > 2$ is occurred in 8.6 times more often for MC-storms than for Ejecta- storms, and in 2.5 times more often for Sheath-storms than for (MC+Ejecta)- driven storms.

Some decreasing of saturation parameter $Q > 1.8$ (10% decreasing of saturation parameter) leads to an increase number of storms driven by ICME (factor 1.2), mainly due to (MC+Ejecta)-driven storms than Sheath-driven storms (factor 1.37); also it leads to increasing number of Ejecta- and CIR-storms (with factors 2 and 2.6, respectively). The

criterion $Q > 1$ is performed for 2/3 of all ICME- storms versus 1/3 of CIR- and IND- storms, and for almost all Sh_{MC} - and MC- storms (80%).

4. Discussion

Obtained results not only confirm the conclusions of the work [Borovsky and Denton, 2006] that the storms driven by ICME(MC+ Ejecta+ Sheath) the most often satisfy criterion of CPCP saturation, but also we obtained indications that the most often the CPCP saturation is associated with magnetic storms driven by Sheath ($Sh_{MC} + Sh_E$) than by (+Ejecta) (21.5% in comparison with 8.6%, respectively). The occurrence rate of CPCP saturation for Sheath-driven storms is comparable with occurrence rate of saturation for MC-driven storms (21.5% in comparison with 25%, respectively). Thus during the main phase of magnetic storms the values of saturation parameter Q , Alfvén velocity V_a , and proxy Pederson conductivity $\Sigma_p \sim F10.7^{1/2}$ change in dependence on type of SW stream with the largest difference between them for CIR-driven storms and subtypes Sh_{MC} - and MC- driven storms.

In contrast to paper by Borovsky and Denton [2006] we found saturation separately for different parts of ICME: MC and Ejecta, Sheath before MC and Ejecta.

The obtained results are not a surprise and may be explained by changing of SW parameters inside different types of SW streams which induced the magnetic storms. Also the occurrence rate of magnetic storms, induced by ICME, is higher near the maximum phase of solar activity when solar radio emission is stronger and ionospheric conductivity is higher. While the occurrence rate for CIR- driven magnetic storms is higher near the minimum phase of solar activity when solar radio emission is lower.

The Q values are dependent not only on variation of Va but also on Σ_p variation. But on average contribution of Va is greater than contribution of Σ_p (see Table 2). On average the contribution of Va in value of saturation parameter Q exceeds the contribution of the solar radio emission almost an order of magnitude (factor 7-9).

Figure 3 shows the saturation parameter Q versus Va and Q versus $F10.7^{1/2}$ for 4 types of SW streams CIR, MC, MC+Ejecta, Sheath(= $Sh_{MC} + Sh_E$).

For all 4 types of SW the dependence of saturation parameter Q on Alfvénic velocity Va is linear with high coefficients of correlation (changes between $r=0.92$ for CIR-storms and $r=0.97$ for MC-storms). Coefficient of determination equals $r^2 = 0.94$ for MC-driven storms and $r^2=0.84$ for CIR-storms, that is about 94% and 84% variations of Q and Va are common for magnetic storms driven by MC and CIR, respectively. While linear dependence of the saturation parameter Q on the solar radio flux $F10.7^{1/2}$ (proxy Σ_p) is weaker (coefficients of correlation change between $r=0.61$ for CIR-storms and $r=0.15$ for MC-storms). Thus only 2% and 5% of the variations in Q and in $F10.7^{1/2}$ are common for MC- and MC+Ejecta- storms, respectively; and 20% and 37% of variations of both parameters are common for Sheath - and CIR- storms, respectively. The strong linear dependence of Q on Va with high values of correlation coefficients during magnetic storms driven by all types of SW may be explained by more large contribution of Va in value of parameter Q in comparison with ionospheric conductivity.

As it is seen in Figure 3 a necessary condition for fulfilment of saturation criteria $Q > 2$ is not only high Alfvénic velocity of SW ($Va > 125 - 150$ km/s), that is high dayside reconnection rate, but also large ionospheric conductivity Σ_p (range changing of solar

radio flux $F10.7^{1/2} \sim 10 - 17$ corresponds to variation of conductivity $\Sigma_p \sim 7.7 - 13.1$ S). Contribution of each of these terms in the Q value depends on the type of SW stream.

We can assume that 80% of saturation can be explained by the processes external magnetosphere-ionosphere system [Ridley, 2005]. The high Alfvén velocity V_a means more efficient reconnection between interplanetary magnetic field at the dayside of magnetosphere. On the other hand V_a connected with Mach number $Ma(\sim V/V_a)$. The dependence of Q versus Ma (not presented here) show that criteria of saturation ($Q > 2$) corresponds to the low values of Mach number (< 4.5) for all types of magnetic storms.

It should be noted that we used in our calculations the solar radio flux $F10.7^{1/2}$ as proxy integrated Pederson conductivity Σ_p . The real system of field aligned currents also includes currents zone 2, but usually it not presented in MHD models (e.g., [Raeder et al., 1998]). Further investigations are required.

5. Conclusions

By using the model of Siscoe-Hill [Hill et al., 1976; Siscoe et al., 2002a, b, 2004; Siscoe, 2011] we evaluate criteria of the CPCP saturation (parameter saturation $Q = V_a F10.7^{1/2} / 1050 > 2$) during the main phases of 257 magnetic storms ($Dst_{min} \leq -50$ nT) induced by the following types of the solar wind streams: corotating interaction regions, CIR – 56 magnetic storms; magnetic clouds, MC – 24 magnetic storms; the compression regions ahead MC, Sh_{MC} – 5 events; Ejecta – 69 events; the compression regions ahead Ejecta, Sh_E – 46 events, and indeterminate type IND (the sources which are impossible to determine because of data gap) – 57 events. Also we calculate similar parameters for sum of subtypes of ICME, magnetic clouds MC and Ejecta (MC+Ejecta)

– 93 magnetic storms, and compression regions before them Sheath ($Sh_{MC} + Sh_E$) – 51 magnetic storms.

We obtained and analyzed the occurrence distribution of saturation parameter Q values, of the Alfvén velocity Va and of solar radio flux $F10.7^{1/2}$ (as proxy height-integrated Pederson conductivity Σ_p) according type of solar wind drivers.

The median values of Q depend on type of magnetic storms and change in ~ 2.8 - 1.8 times between maximal values for Sh_{MC} - and MC- storms and minimal values for CIR-storms. The median value Q is higher in ~ 1.6 times for Sh_{MC} - storms than for MC-storms.

The median values of Va are changing in 1.4 - 1.8 times between maximum values for ShE- and MC-storms and minimal values for CIR- and Ejecta- storms, respectively. For storms induced by MC and Sh_{MC} the factor between median values Va is ~ 1.3 .

The median values of solar radio flux $F10.7^{1/2}$ change in 1.3 times between maximum values for Sh_{MC} - storms and minimal values $F10.7^{1/2}$ for CIR-storms. The median values $F10.7^{1/2}$ are larger in ~ 1.2 times for Sh_{MC} - storms than for MC-storms.

Thus we obtained that during the main phase of magnetic storms the values of saturation parameter Q , Alfvén velocity Va , and proxy Pederson conductivity $\Sigma_p \sim F10.7^{1/2}$ change in dependence on type of SW stream with the largest difference between them for CIR-driven storms and subtypes Sh_{MC} - and MC- driven storms.

The saturation parameters Q values are dependent on variations of both parameters as Alfvénic velocity Va as ionospheric conductivity Σ_p . But on average the contribution of Va in value of saturation parameter Q exceeds in ~ 7 - 9 times the contribution of Σ_p variation of the solar radio emission $F10.7^{1/2} (\sim \Sigma_p)$.

Our analysis allows us to make following main conclusions.

1) On the main phase of magnetic storms the CPCP saturation depends on type of the solar wind stream induced the magnetic storm.

2) The saturation criterion ($Q > 2$) of the CPCP is performing mainly for strong magnetic storms initiated by ICME(MC+Ejecta+Sheath) (13.2% storms), and in ~ 3.5 times rarely for CIR- and IND- storms (3.5%).

3) Most often saturation criterion ($Q > 2$) of cross polar cap potential is satisfied for storms driven by MC (25%) than by Ejecta (2.9%);

4) The saturation ($Q > 2$) of cross polar cap potential in 2.5 times more often is satisfied for Sheath- storms (21.5%) than for storms driven by sum of MC+Ejecta (8.6%);

5) Decreasing of saturation level on 10% ($Q > 1.8$) increases the number of ICME-storms with the CPCP saturation to 20% (by 40% due to storms driven by sum of MC+Ejecta and by 9% due to storms driven by Sheath).

Acknowledgments. The authors are grateful for the possibility of using the OMNI database. The OMNI data were obtained from the GSFC/SPDF OMNIWeb on the site <http://omniweb.gsfc.nasa.gov>. This work was supported by the Russian Foundation for Basic Research (RFBR), project 13-02-00158a, and by the Program 22 of Presidium of Russian Academy of Sciences.

References

Balan N., Bailey G. J., Jayachandran B. (1993), Ionospheric evidence for a nonlinear relationship between the solar e.u.v. and 10.7 cm fluxes during an intense solar cycle, Planet. Space Sci., V.41,. N.2. P. 141–145.

- Borovsky, J. E. and Denton, M.H. (2006), Differences between CME-Driven Storms and CIR-Driven Storms, *J. Geophys. Res.*, 28, 121–190.
- Borovsky, J. E., B. Lavraud, and M. M. Kuznetsova (2009), Polar cap potential saturation, dayside reconnection, and changes to the magnetosphere, *J. Geophys. Res.*, 114, A03224, doi:10.1029/2009JA014058.
- Boudouridis, A., E. Zesta, L. R. Lyons, and P. C. Anderson, (2004), Evaluation of the Hill-Siscoe transpolar potential saturation model during a solar wind dynamic pressure pulse, *Geophys. Res. Lett.*, 31, L23802, doi:10.1029/2004GL021252.
- Burlaga, L. F., Sittler E., Mariani F., and Schwenn R., Magnetic loop behind an interplanetary shock: Voyager, Helios, and IMP 8 observations, *J. Geophys. Res.*, 86, p. 6673–6684, 1981.
- Despirak, I.V., Lubchich, A.A., and Guineva, V., Development of substorm bulges during storms of different interplanetary origins, *J. of Atmosph. and Sol. Terrest. Phys.*, 2011, vol. 73, p. 1460–1464.
- Floyd L., Newmark J., Cook J., Herring L., McMullin D. (2005), Solar EUV and UV spectral irradiances and solar cycles, *J. Atmos. Sol. Terr. Phys.* V. 67, P. 3–15.
- Gao Ye, Kivelson Margaret G., Walker Raymond J., Two Models of Cross Polar Cap Potential Saturation Compared: Siscoe-Hill model versus Kivelson-Ridley model , *JGR*, 2013, doi:10.1002/jgra.50124.
- Guo, J., Feng, X., Emery, B.A., et al., Energy transfer during intense geomagnetic storms driven by interplanetary coronal mass ejections and their sheath regions, *J. Geophys. Res.*, 2011, vol. 116, A05106. doi:10.1029/2011JA016490.

- Hairston, M. R., Hill T. W., and Heelis R. A., (2003), Observed saturation of the ionospheric polar cap potential during the 31 March 2001 storm, *Geophys. Res. Lett.*, 30(6), 1325, doi:10.1029/2002gl015894.
- Hairston, M. R., K. A. Drake, and R. Skoug (2005), Saturation of the ionospheric polar cap potential during the October–November 2003 superstorms, *J. Geophys. Res.*, 110, A09S26, doi:10.1029/2004JA010864.
- Hernandez, S., R. E. Lopez, M. Wiltberger, and J. G. Lyon (2007), MHD simulations of solar wind-geospace coupling, *Eos Trans. AGU*, 88(23), Spring Meet. Suppl., Abstract SM51C 03.
- Hill T.W., Dessler A.J., Wolf R.A. (1976), Mercury and Mars: the role of ionospheric conductivity in the acceleration of magnetospheric particles, *Geophys. Res. Lett.*, V.3., N. 8., P. 429–432.
- Huttunen, K.E.J., Koskinen, H.E.J., Karinen, A., and Mursula, K., Asymmetric development of magnetospheric storms during magnetic clouds and sheath regions, *Geophys. Res. Lett.*, 2006, vol. 33, p. L06107. doi: 10.1029/2005GL027775.
- King, J. H., and N. E. Papitashvili (2005), Solar wind spatial scales in and comparisons of hourly Wind and ACE plasma and magnetic field data, *J. Geophys. Res.*, 110, A02104, doi:10.1029/2004JA010649.
- Kivelson, M. G., and Ridley A. J., (2008), Saturation of the polar cap potential: Inference from Alfvén wing arguments, *J. Geophys. Res.*, 113(A5), A05214, doi:10.1029/2007ja012302.
- Lavraud Benoit and Borovsky Joseph E., (2008), Altered solar wind - magnetosphere interaction at low Mach numbers: coronal mass ejections, *Journal of Geophysical Research*

113, CiteID A00B08” DOI : 10.1029/2008JA013192.

Longden N., Denton M.H. and Honary F., Particle precipitation during ICME-driven and CIR-driven geomagnetic storms, *J. Geophys. Res.*, 2008, vol. 113, p. A06205. doi:10.1029/2007JA012752.

Merkine, V. G., Papadopoulos K., Milikh G., Sharma A. S., Shao X., Lyon J., and Goodrich C., (2003), Effects of the solar wind electric field and ionospheric conductance on the cross polar cap potential: Results of global MHD modeling, *Geophys. Res. Lett.*, 30(23), 2180, doi: 10.1029/2003gl017903.

Merkin, V. G., Sharma A. S., Papadopoulos K., Milikh G., Lyon J., and Goodrich C., (2005a), Global MHD simulations of the strongly driven magnetosphere: Modeling of the transpolar potential saturation, *J. Geophys. Res.*, 110, A09203, doi:10.1029/2004JA010993.

Merkin V. G., Sharma A. S., Papadopoulos K., Milikh G., Lyon J., and Goodrich C., (2005b), Relationship between the ionospheric conductance, field aligned current, and magnetopause geometry: Global MHD simulations, *Planet. Space Sci.*, 53, 873–879, doi:10.1016/j.pss.2005.04.001.

Nagatsuma T. (2002), Saturation of polar cap potential by intense solar wind electric fields, *Geophys. Res. Lett.*, 29(10), 1422, doi: 10.1029/2001gl014202.

Nikolaeva, N. S., Yu. I. Yermolaev, and I. G. Lodkina, (2011), Dependence of Geomagnetic Activity during Magnetic Storms on the Solar Wind Parameters for Different Types of Streams, *Geomagnetism and Aeronomy*, Vol. 51, No. 1, pp. 49–65. (*Geomagnetizm i Aeronomiya*, 2011, Vol. 51, No. 1, pp. 51–67.)

- Ober D. M., Maynard N. C., Burke W. J. (2003), Testing the Hill model of transpolar potential saturation, *J. Geophys. Res.* V. 108, N. A12, P. 1467, doi:10.1029/2003JA010154.
- Plotnikov, I. Ya. and Barkova, E.S., (2007), Nonlinear Dependence of Dst and *AE* Indices on the Electric Field of Magnetic Clouds, *Adv. Space Res.*, vol. 40, p. 1858–1862.
- Pudovkin, M. I., S. A. Zaitseva, T. A. Bazhenova, and V. G. Andrezen (1985), Electric fields and currents in the Earths polar caps, *Planet. Space Sci.*, 33, 407414, doi:10.1016/0032-0633(85)90085-6.
- Pulkkinen T. I., Partamies N., Huttunen K. E. J., Reeves G. D., and Koskinen H. E. J.: Differences in geomagnetic storms driven by magnetic clouds and ICME sheath regions, *Geophys. Res. Lett.*, 34, L02105, doi:10.1029/2006GL027775, 2007.
- Raeder J., Berchem J., Ashour-Abdalla M., The Geospace Environment Modeling Grand Challenge: Results from a Global Geospace Circulation Model, *Journal of Geophysical Research: Space Physics*, V. 103, Iss. A7, pages 1478714797, 1998.
- Raeder, J., Wang Y. L., Fuller -Rowell T. J., and Singer H. J., (2001), Global simulation of magnetospheric space weather effects of the Bastille day storm, *Sol. Phys.*, 204(1-2), 323-337, doi:10.1023/A:1014228230714.
- Raeder J., and Lu G., (2005), Polar cap saturation during large geomagnetic storms, *Adv. Space Res.*, 36, p.1804.
- Ridley A. J. (2005), A new formulation for the ionospheric cross polar cap potential including saturation effects, *Ann. Geophys.*, 23(11), p.3533–3547, doi: 10.5194/angeo-23-3533-2005.
- Ridley, A. J. (2007), Alfvén wings at Earths magnetosphere under strong interplanetary magnetic fields, *Ann. Geophys.*, 25, p.533.

- Reiff P. H., and J. G. Luhmann. (1986), Solar wind control of the polar-cap voltage, in *Solar Wind-Magnetosphere Coupling*, edited by Kamide Y., Slavin J. A. Terra Sci. Tokyo. P. 453–476.
- Robinson R.M., Vondrak R.R. (1984), Measurements of E region ionization and conductivity produced by solar illumination at high latitudes, *J. Geophys. Res.* V.89. P. 3951–3956.
- Russell C. T., Lu G., and Luhmann J. G., (2000), Lessons from the ring current injection during the September 24, 25, 1998 storm, *Geophys. Res. Lett.*, 27(9), p.1371–1374, doi: 10.1029/1999gl003718.
- Russell C. T., Luhmann J. G., and Lu G., (2001), Nonlinear response of the polar ionosphere to large values of the interplanetary electric field, *J. Geophys. Res.*, 106, p.18495–18504, doi:10.1029/2001JA900053.
- Siscoe, G. L., Erickson, G. M., Sonnerup, B. U. O., Maynard, N. C., Schoendorf, J. A., Siebert, K. D., Weimer D. R., White W. W., and Wilson G. R., Hill model of transpolar potential saturation: Comparisons with MHD simulations, (2002a), *J. Geophys. Res.* 107(A6), 1075, doi10.1029/2001JA000109.
- Siscoe, G. L., Crooker N. U., Siebert K. D. (2002b), Transpolar potential saturation: Roles of region 1 current system and solar wind ram pressure, *J. Geophys. Res.* V. 107, A10, P. 1321, doi:10.1029/2001JA009176.
- Siscoe, G. L., G. M. Erickson, B. U. O? . Sonnerup, N. C. Maynard, J. A. Schoendorf, K. D. Siebert, D. R. Weimer, W. W. White, and G. R. Wilson (2002a), Hill model of transpolar potential saturation: Comparisons with MHD simulations, *J. Geophys. Res.*, 107(A6), 1075, doi:10.1029/ 2001JA000109.

Siscoe G., Rader J., Ridley A. J. (2004), Transpolar potential saturation models compared // J. Geophys. Res. V. 109. A09203. doi:10.1029/2003JA010318.

Siscoe G., (2011), Aspects of global coherence of magnetospheric behavior, Journal of Atmospheric and Solar-Terrestrial Physics, 73 , 402–419

Shepherd S. G., Greenwald R. A., and Ruohoniemi J. M., (2002), Cross polar cap potentials measured with Super Dual Auroral Radar Network during quasi-steady solar wind and interplanetary magnetic field conditions, J. Geophys. Res., 107(A7), 1094, doi: 10.1029/2001ja000152.

Shepherd S.G., (2007), Polar cap potential saturation: Observations, theory, and modeling, Journal of Atmospheric and Solar-Terrestrial Physics, 69, 234–248.

Turner, N.E., Cramer, W.D., Earles, S.K., and Emery, B.A., Geoefficiency and energy partitioning in CIR-driven and CME-driven storms, J. of Atmosph. and Sol.-Terrest. Phys., 2009, vol. 71, pp. 1023–1031.

Winglee R. M., Chua D., Brittnacher M. and Parks G. K., (2002), Global impact of ionospheric outflows on the dynamics of the magnetosphere and cross-polar cap potential, J. Geophys. Res., 107(A9), p.1237, doi:10.1029/2001JA000214.

Yermolaev Yu. I., Yermolaev M. Yu., Nikolaeva N. S., and Lodkina L. G. (2007), Interplanetary conditions for CIR-induced and MC- induced geomagnetic storms, Bulg. J. Phys., 34, p.128–135.

Yermolaev, Yu. I., et al., (2009), Catalog of Large-Scale Solar Wind Phenomena during 1976-2000, Kosm. Issled., vol. 47, no. 2, pp. 99–113. [Cosmic Research, pp. 81–94].

Yermolaev Yu. I., N. S. Nikolaeva I. G. Lodkina, and Yermolaev M. Yu., (2010), Relative Occurrence Rate and Geoeffectiveness of Large-Scale Types of the Solar Wind, Kos-

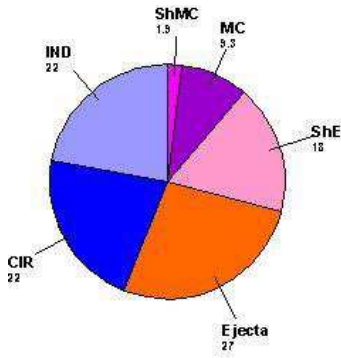


Figure 1. The distribution of magnetic storms with $Dst \leq -50$ nT in dependence on type of the solar wind driver (in %).

Table 1. Average and median values of Va , Q , $F10.7^{1/2}$ for magnetic storms induced by different types of SW.

Type of SW	Number of storms	Va Average	Va Median	$F10.7^{1/2}$ Average	$F10.7^{1/2}$ Median	Q Average	Q Median
MC	24	134.9	112	12.98	13.45	1.65	1.53
CIR	56	84.2	78	12	12.5	0.98	0.85
Ejecta	69	85.8	78	13.18	13.56	1.08	0.96
Sh_E	46	99.7	95	13.1	13.5	1.2	1.2
Sh_{MC}	5	140.7	145	15.6	16	2.12	2.4
Sheath ($Sh_{MC} + Sh_E$)	51	104	96	13.3	13.5	1.33	1.2
MC+Ejecta	93	98.5	98.5	13.1	13.5	1.2	1.2
IND	57	76.4	70	12.8	13.5	0.94	0.91
ICME (MC+Ejecta+Sheath)	144	100.3	93.5	13.2	13.55	1.26	1.2

micheskie Issledovaniya, Vol. 48, No. 1, pp. 3–32. (Cos. Res., 2010, Vol. 48, No. 1, pp. 1–30).

Yermolaev Y. I., Nikolaeva N. S., Lodkina I. G. and Yermolaev M. Y., (2012), Geoeffectiveness and efficiency of CIR, sheath, and ICME in generation of magnetic storms, J. Geophys. Res., 117, A00L07, doi:10.1029/2011JA017139.

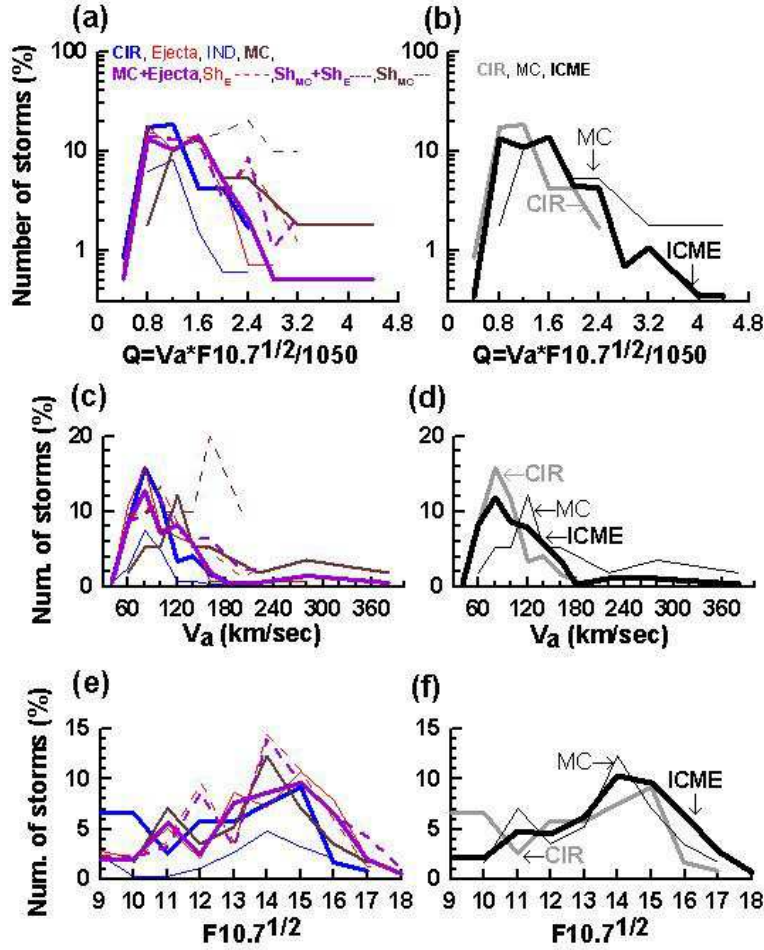


Figure 2. Distributions of Q , Va , $F10.7^{1/2}$ for different types/subtypes of SW drivers. Panels (b, d, f) give the same distributions only for 3 types of SW drivers: CIR, MC, and ICME (= MC + Ejecta + Sheath).

Table 2. The number of magnetic storms driven by various types of SW for 3 levels of saturation parameter Q .

Type of SW	Number of storms	N with $Q > 2$, (% of storms)	N with $Q > 1.8$, (% of storms)	N with $Q > 1$, (% of storms)
MC	24	6 (25%)	7 (29%)	20 (83%)
CIR	56	2 (3.5%)	5 (9%)	21 (37.5%)
Ejecta	69	2 (2.9%)	4 (5.8%)	32 (46.4%)
Sh_E	46	7 (15%)	8 (17.4%)	27 (58.7%)
Sh_{MC}	5	4 (80%)	4 (80%)	4 (80%)
Sheath ($Sh_{MC} + Sh_E$)	51	11 (21.5%)	12 (23.5%)	31 (61%)
MC+Ejecta	93	8 (8.6%)	11 (11.8%)	52 (56%)
IND	57	2 (3.5%)	2 (3.5%)	19 (33%)
ICME (MC+Ejecta+Sheath)	144	19 (13.2%)	23 (16%)	83 (57.6%)

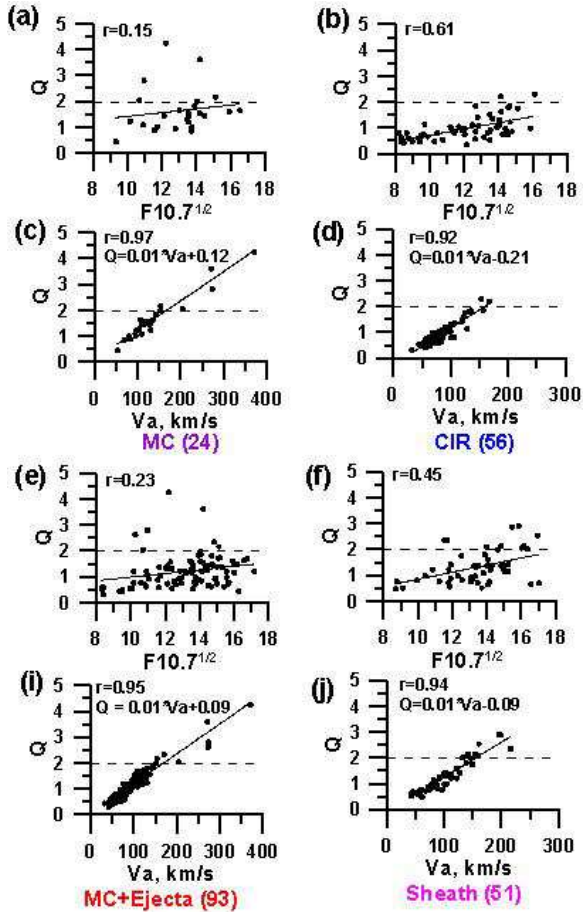


Figure 3. A saturation parameter Q versus Va (c, d, i, j) and Q versus $F10.7^{1/2}$ (a, b, e, f) for 4 types of magnetic storms induced by SW streams: MC (a, c), CIR (b, d), sum of (MC+Ejecta) (e, i), and Sheath ($Sh_{MC} + Sh_E$) before (MC+Ejecta) (f, j).